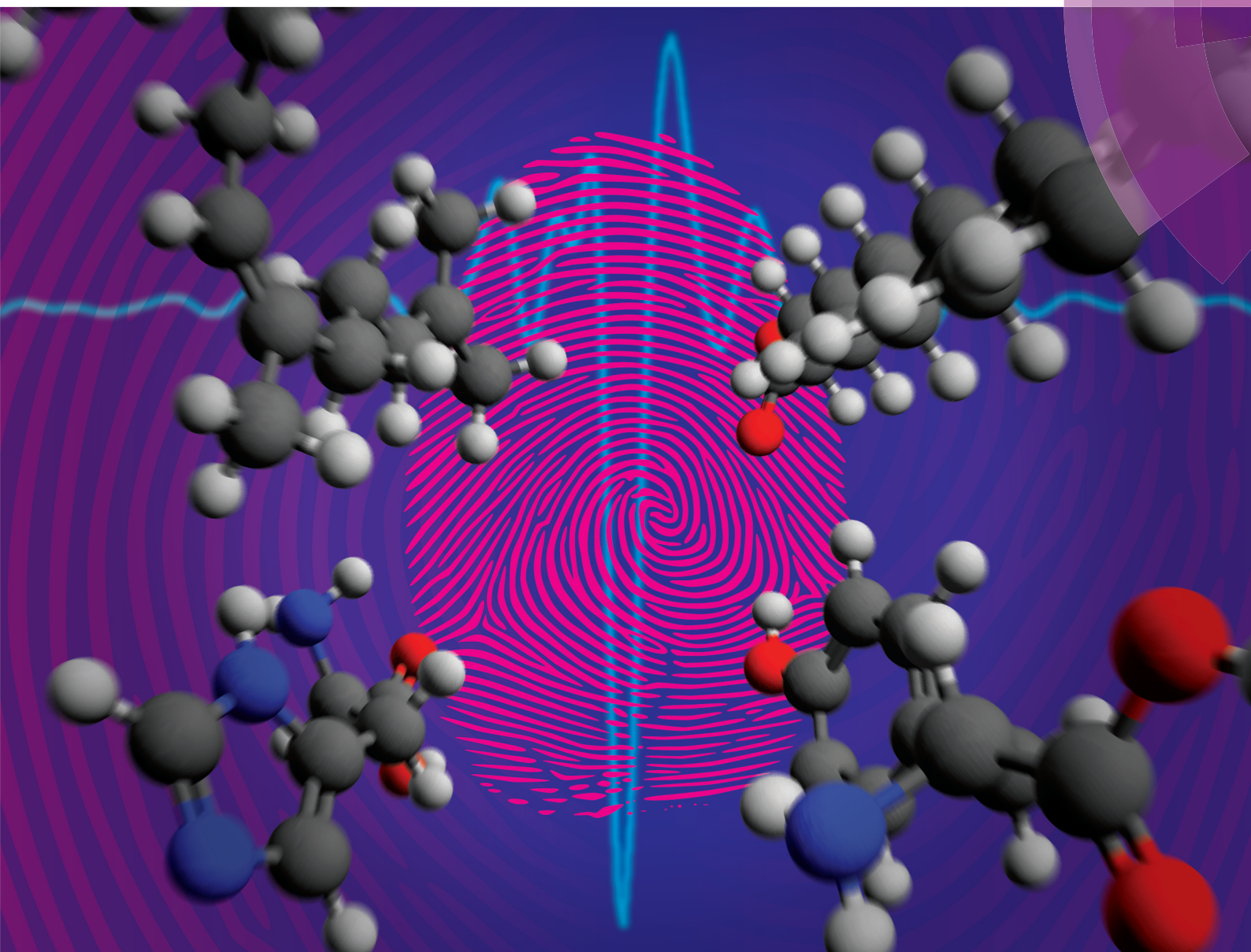


# Analyst

rsc.li/analyst



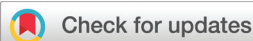
ISSN 0003-2654



**PAPER**

Mark J. Hackett, Simon W. Lewis *et al.*

Revealing the spatial distribution of chemical species within latent fingerprints using vibrational spectroscopy



Cite this: *Analyst*, 2018, **143**, 4027

## Revealing the spatial distribution of chemical species within latent fingerprints using vibrational spectroscopy†

Buddhika N. Dorakumbura,<sup>a,b</sup> Rhiannon E. Boseley,<sup>a,b</sup> Thomas Becker,<sup>a,b</sup> Danielle E. Martin,<sup>c</sup> Andrea Richter,<sup>d</sup> Mark J. Tobin,<sup>c</sup> Wilhelm van Bronswijk,<sup>a</sup> Jitraporn Vongsivut,<sup>c</sup> Mark J. Hackett<sup>a,b</sup> and Simon W. Lewis<sup>a,b</sup>

Latent fingerprints are an important form of crime-scene trace evidence and their usefulness may be increased by a greater understanding of the effect of chemical distribution within fingerprints on the sensitivity and robustness of fingerprint detection methods. Specifically, the relative abundance and micro-distribution of sebaceous (lipophilic) and eccrine (hydrophilic) material in fingerprints have long been debated in the field, yet direct visualisation of relative abundance and micro-distribution was rarely achieved. Such a visualisation is nonetheless essential to provide explanations for the variation in reproducibility or robustness of latent fingerprint detection with existing methods, and to identify new strategies to increase detection capabilities. In this investigation, we have used SR-ATR-FTIR and confocal Raman microscopy to probe the spatial micro-distribution of the sebaceous and eccrine chemical components within latent fingerprints, deposited on non-porous surfaces. It was determined that fingerprints exhibit a complex spatial distribution, influenced by the ratio of lipophilic to aqueous components, and to a first approximation resemble a water-in-oil or oil-in-water emulsion. Detection of a substantial lipid component in "eccrine enriched fingerprints" (wherein hands are washed to remove lipids) is noteworthy, as it provides a potential explanation for several scenarios of unexpected fingerprint detection using methods previously thought unsuitable for "eccrine deposits". Furthermore, the pronounced distribution of lipids observed in natural fingerprint deposits was intriguing and agrees with recent discussion in this research field that natural fingerprints contain a much higher lipid content than previously thought.

Received 29th September 2017,  
Accepted 11th June 2018

DOI: 10.1039/c7an01615h

rsc.li/analyst

## Introduction

Latent fingerprints are trace quantities of skin secretions and cellular debris that are transferred to a surface during finger to surface contact. Successful detection of these trace chemical components reveals the fingerprint impression, and is a cornerstone of forensic investigations. Unfortunately, not all latent fingerprints can be detected with current techniques, and a significant number of deposits remain undetected due to issues of sensitivity and specificity.<sup>1</sup> A more comprehensive

knowledge of the fingerprint deposit itself would be advantageous in the pursuit of improved fingerprint detection capabilities and would retrieve additional information from the recovered deposit.

The composition of latent fingerprints is a mixture of water-soluble and water-insoluble components originating from the eccrine and sebaceous glands of the skin, skin debris, and residues of materials that have been handled prior to deposition. Herein, we shall refer to water-soluble (hydrophilic) chemical components and water-insoluble (lipophilic) chemical components as eccrine and sebaceous material, respectively. There have been a number of investigations of the bulk chemical composition of fingerprints,<sup>2–7</sup> yet the spatial distribution of eccrine and sebaceous chemical components within the deposit is less well understood. Fingerprint composition is often characterised by bulk measurement techniques such as GC-MS and LC-MS.<sup>2–4,6,8</sup> Although bulk methods do not reveal spatial distribution, they have provided an important insight into time-course chemical alterations that occur in fingerprints following deposition. Supported by their GC-MS

<sup>a</sup>School of Molecular and Life Sciences, Curtin University, GPO Box U1987, Perth, Western Australia 6845, Australia. E-mail: S.Lewis@curtin.edu.au, mark.j.hackett@curtin.edu.au

<sup>b</sup>Curtin Institute of Functional Molecules and Interfaces, GPO Box U1987, Perth, Western Australia 6845, Australia

<sup>c</sup>Australian Synchrotron, 800 Blackburn Road, Clayton, Victoria 3168, Australia

<sup>d</sup>WITec GmbH, Lise-Meitner-Strasse 6, 89081 Ulm, Germany

†Electronic supplementary information (ESI) available. See DOI: 10.1039/c7an01615h



analysis, Mong *et al.* postulated a series of processes that may take place over time in the fingerprint residue, to account for apparent hardening of the fingerprint and resistance to partitioning by development reagents.<sup>2</sup> They postulated that the surface of the fingerprint residue developed a waxy coating with age-since-deposition, due to the evaporation of water and transformation of unsaturated compounds to saturated analogues. This layer may hinder the ability of residue components to interact with development reagents by decreasing the surface area for contact.<sup>2</sup> Four decades ago, Thomas *et al.* emphasised the importance of knowledge of the spatial distribution of fingerprint components to understand and interpret any physical measurements on latent fingerprint deposits.<sup>9</sup> For example, Moret *et al.* observed fingerprint ridge impressions on glass four days following deposition.<sup>1</sup> Fingermarks deposited on PVC, however, were no longer observable. This could be due to variation in chemical distribution within the fingerprint and interactions of the chemical distribution with the substrate.<sup>1</sup> Surface tension and modifications of non-porous surfaces are thought to be causative factors, contributing to the results of Moret *et al.*, but this hypothesis is still under investigation.<sup>1</sup> The interactions between hydrophilic and hydrophobic fingerprint components with non-porous substrates may also influence the distribution, subsequently influencing the degradation over time. In order to gain a better understanding of the observations discussed above, advanced characterisation of the spatial distribution of chemical components within the eccrine and sebaceous secretions of a fingerprint deposit is required. Non-destructive, direct chemical imaging techniques hold great potential in this respect.

FTIR and Raman spectroscopy are ideal for non-destructive characterisation of latent fingerprints due to their ability to directly image (map) chemical components at micron scales.<sup>10,11</sup> While other techniques such as MALDI-MSI are more sensitive and may offer greater chemical specificity,<sup>12,13</sup> FTIR and Raman provide superior spatial resolution, which is essential to study the distribution of eccrine and sebaceous components across the deposit. FTIR spectroscopy has been used in previous research to detect fingerprints on different substrates, deduce donor traits such as age and gender and to estimate the time since deposition.<sup>5,10,14–20</sup> Despite the relative improvement of spatial resolution obtained with FTIR compared to other methods, the spatial resolution is still hampered by the long wavelengths of light used relative to optical microscopy. Furthermore, traditional transmission FTIR limits analyses to fingerprints deposited on infrared-transparent substrates (which are relatively rare, expensive, and are not likely to feature at a crime scene). One alternative is to use attenuated total reflectance FTIR (ATR-FTIR), which improves spatial resolution and enables measurement of fingerprints deposited on infrared-opaque substrates (such as glass). Such advantages were demonstrated by Ricci *et al.* to directly measure and reveal the chemical and spatial information of primarily sebaceous components in fingerprints.<sup>15</sup> Recently, Fritz *et al.* demonstrated the advantages of synchrotron radiation as the

infrared source to deliver the best possible spatial resolution, with adequate signal to noise ratio, in a shortened experimental time-frame (compared to a non-synchrotron source).<sup>14</sup> The results of Fritz *et al.* suggested that fingerprints were comparatively chemically homogeneous, both within-samples and between-samples. However, such results were interpreted with caution, as only representative spectra were collected. No chemical imaging was acquired on the entire droplets at micron-scale spatial resolution, which otherwise could be used as direct evidence of reported homogeneity. We have recently reported varying surface adhesion within fingerprint droplets using atomic force microscopy (AFM), which suggested possible chemical heterogeneity within individual droplets.<sup>21</sup>

An alternative technique to ATR-FTIR to image fingerprints at micron-spatial resolution is Raman microscopy, which typically provides improved spatial resolutions compared to those achieved using FTIR techniques, due to the use of shorter laser excitation wavelengths. Raman spectroscopy, including surface-enhanced Raman spectroscopy, has been successfully applied to chemical imaging of latent fingerprint ridge patterns and to detect exogenous substances such as illicit drugs and explosive residues.<sup>22–25</sup> However, it has not been applied to the study of the fundamental chemical characteristics of fingerprint deposits. Both FTIR and Raman techniques complement each other, as vibrational modes that are strong in an FTIR spectrum are usually weak in a Raman spectrum and *vice versa*.<sup>26,27</sup> Therefore, they are often used together to gather a more complete chemical picture of a sample.

The work presented here reports the use of synchrotron-based radiation ATR-FTIR microscopy (SR-ATR-FTIR) and confocal Raman microscopy to reveal the relative abundance and distribution of eccrine and sebaceous material in fingerprints at the micron scale. These findings will enable more evidence-based approaches, using non-destructive techniques, to study fingerprint composition and its variation over time.

## Experimental

### Fingerprint deposition

The details of the donors and the types of deposits obtained are listed in Table 1. Donors gently pressed their index fingers down for 10 s on non-porous substrates, which had been pre-cleaned with ethanol.

Zinc selenide slides (Crystran Ltd, UK) and calcium fluoride slides (Crystran Ltd, UK) were used as the non-porous substrates for FTIR studies. Glass cover slides (22 mm × 22 mm, Deckgläser, Germany) were used as substrates for the Raman study. An additional sample was prepared *via* fingerprint deposition directly onto the Ge ATR crystal, which was used as a control experiment to demonstrate that the contact made between the substrate (glass slide) and the Ge crystal did not drastically alter the morphology or chemical distribution within fingerprint droplets (ESI 1 and 2†). For “eccrine deposits”, donors washed their hands with soap and water and waited for 30 min without touching any surfaces prior to



**Table 1** Details of the donors and the deposits analysed during the study

Study	Donor	Type of the deposit	Age (years)	Gender	Cosmetic use
IR and Raman	Donor 1	Natural and eccrine	33	Female	Moisturiser, cosmetics and hand cream
IR	Donor 2	Natural	77	Male	None
IR	Donor 3	Eccrine	48	Male	Moisturiser
IR	Donor 4	Sebaceous	21	Male	None
Raman	Donor 5	Natural and eccrine	26	Male	None
Raman	Donor 6	Natural	32	Female	Moisturiser and cosmetics
Raman	Donor 7	Natural and sebaceous	20	Female	Moisturiser and hand cream
Raman	Donor 8	Natural	23	Female	Moisturiser and cosmetics
Raman	Donor 9	Natural	31	Male	Face cream

deposition. For “natural deposits”, the donor activities were not controlled; however, food handling and hand washing within 30 min prior to deposition were avoided. Fingers were deliberately charged with sebum by rubbing them on the face prior to deposition of the “sebaceous deposits”. At least twelve randomly selected droplets with different shapes and appearance from four areas of the deposit (top two corners and bottom two corners from the centre of the deposit) were analysed during the Raman study. The samples were analysed within 10 min to 5 hours after deposition.

#### Benchtop thermal source FTIR-FPA imaging studies

A larger area of a sebaceous fingermark deposit was investigated in transmission mode using a Bruker Hyperion 3000 FTIR microscope equipped with a liquid nitrogen cooled 64 × 64 pixel focal plane array (FPA) detector and a 15× objective lens (NA = 0.4), coupled to a Bruker Vertex 70 FTIR spectrometer (Bruker Optik, Ettlingen, Germany). A thermal global infrared source was used. Data collection was controlled using Bruker OPUS Software v7.2. The sample chamber was purged with dry nitrogen to reduce the contribution of atmospheric water vapour and CO<sub>2</sub>. Details of the instrumental arrangements for FTIR studies are given in Table 2.

#### Synchrotron sourced FTIR studies

The synchrotron infrared beamline consists of a Bruker Vertex V80v FTIR spectrometer coupled with a Bruker Hyperion 2000 microscope (Bruker Optik GmbH, Ettlingen, Germany) and a liquid nitrogen cooled narrow band mercury cadmium telluride (MCT) detector. A 36× objective and a 36× condenser with a matched numerical aperture (NA = 0.5) were used for data collection. Both the spectrometer and the microscope were continuously purged with dry nitrogen to reduce the interference of water vapour and CO<sub>2</sub> on spectra. The synchrotron beam was focused onto the sample, with a focused beam size of approximately 10 μm diameter (wavelength dependent).

The Hyperion microscope was equipped with pinholes of different sizes (0.15, 0.25, 0.42, 0.60 and 0.75 mm) to further refine the focused beam size and thereby reducing the sampling area from which spectra are recorded. The 0.25 mm pinhole was used for the synchrotron sourced FTIR experiments in transmission mode to achieve a measurement area on the sample 6.9 μm in diameter.

To achieve higher spatial resolution, an in-house developed macro-attenuated total reflection (ATR) accessory equipped with a germanium (Ge) hemispheric ATR crystal ( $n_{\text{Ge}} = 4.0$ ) was used to produce diffraction limited spatial resolution with a fourfold improvement relative to an equivalent transmission measurement. Furthermore, coupling of the synchrotron beam into the hemispherical crystal resulted in a fourfold decrease in the mapping step size relative to the physical step size motion of the sample stage (*i.e.*, a 2 μm motor step size produces a 0.5 μm translation of the synchrotron beam at the sample/ATR interface). The term “macro” in macro-ATR refers to the macro-sized area of the Ge crystal that makes contact with the sample, enabling larger sample areas to be imaged at micron spatial resolution (the technique, in essence though, is a form of micro-spectroscopy).

All the raw FTIR spectra were baseline corrected and analysed using Bruker OPUS v7.2 and CytoSpec 2.00.01 software (Cytospec Inc., Boston, MA, USA). Images were further processed with ImageJ 1.50i software.

#### Confocal Raman microscopy

Confocal Raman microscopy was performed using a confocal Raman microscope (alpha 300R, WITec, Ulm, Germany) equipped with a frequency doubled Nd:YAG laser (532 nm) and a piezo scanner operating under following settings: 100× objective, NA 0.9. The spatial resolution of the instrument in this configuration is 300 nm and is diffraction limited according to Rayleigh theory. The sample is mounted onto a piezo-driven scanning stage with a position accuracy <2 nm in the

**Table 2** Details of the instrumental setup for FTIR studies

IR source	Acquisition mode and the detector	Objective	NA	Scans	Spectral resolution (cm <sup>-1</sup> )	Pinhole size (mm)	Pixel size (μm)
Thermal global	Transmission, FPA detector	15×	0.4	256	4	—	21.3
Synchrotron	Transmission, MCT detector	36×	0.5	256	4	0.25	2.5
Synchrotron	Macro ATR, MCT detector	20×	0.6	4	8	0.15	0.25



*x* and *y* directions. The spectra were acquired with a thermoelectrically cooled CCD detector placed behind the spectrometer at a spectral resolution of 3 cm<sup>-1</sup>. The WITec Control FOUR software was used for data acquisition and WITec Project FOUR 4.1 for spectral processing. Raman images were acquired with 0.1 s integration time per pixel (*i.e.*, 250 nm step size, to yield a 250 nm × 250 nm pixel). After performing a smoothing for cosmic ray removal, the background was removed by subtracting a polynomial fit to raw spectra.

## Results and discussion

### Characterisation of spectroscopic markers of sebaceous and eccrine chemical compounds in fingermarks

The bulk chemical composition of fingermarks has been extensively studied, revealing that the composition of fingermarks is complex (many chemical species present),<sup>2,8,28,29</sup> varied (composition is influenced by the donor,<sup>2,20,29,30</sup> the substrate<sup>1,31</sup> and the environment);<sup>3,4,15,20</sup> and dynamic (composition changes over time).<sup>2-4,32</sup> Despite this complexity, the chemical components of fingermarks can be broadly divided into 3 categories: sebaceous material (lipophilic chemical compounds), eccrine material (hydrophilic chemical compounds), and debris such as skin cells or exogenous particles (cosmetics, dirt, *etc.*). Typical sebaceous, eccrine and debris components of fingermarks are presented in Tables 3 and 4.

Although the bulk composition of fingermarks is well characterised, the distribution of eccrine and sebaceous chemical components within the fingermark is less well known, especially at the micron-scale.<sup>1</sup> A variety of detection methods exist to visualise ridge detail in latent fingermarks; however, few microscopy methods provide the ability to simultaneously visualise and differentiate between the eccrine and sebaceous chemical components. In this study we have sought to fill this gap of knowledge using the direct spectroscopic imaging techniques of infrared microscopy (IRM) and Raman microscopy to characterise the distribution of sebaceous (lipo-

philic) components and eccrine (hydrophilic) components within fingermarks, at the meso-scale (20 μm spatial resolution) and micron-scale spatial resolution. To enable visualisation of sebaceous and eccrine components using IRM and Raman microscopy, we first determined spectroscopic marker bands of sebaceous and eccrine material and ensured that these bands are in good agreement with the published literature.

To determine characteristic spectroscopic marker bands of sebaceous and eccrine material, FTIR and Raman spectra were collected from “natural” fingermarks and “eccrine” fingermarks. “Natural” fingermarks contain a mixture of sebaceous and eccrine material, whereas “eccrine” fingermarks are those deposited from freshly washed hands with a typical time interval of approximately 15–30 min prior to deposition.<sup>13,21</sup> There are no known sebaceous (lipid-secreting) glands on the hand.<sup>33</sup> Therefore, fingermarks deposited following hand-washing contain a lower lipid content, and are enriched in eccrine material relative to natural fingermarks. A comparison of FTIR spectra (Fig. 1A) and Raman spectra (Fig. 1B) collected from “natural” and “eccrine” fingermarks reveals key spectroscopic features that can be used as spectroscopic markers to image the distribution of sebaceous and eccrine material within a fingermark.

### Investigating the distribution of eccrine and sebaceous material across fingermark ridges at the meso-scale

The primary objective of this study was to investigate the distribution of eccrine and sebaceous material within fingermark ridges at the micro-scale. However, due to the established heterogeneity of bulk fingermark chemical composition,<sup>34,35</sup> we first investigated the distribution of eccrine and sebaceous material at the meso-scale (20 μm) using FTIR-spectroscopic imaging (Fig. 2). Specifically, eccrine regions of the fingermark were visualised using the integrated area under the band for the band centred at 1600 cm<sup>-1</sup> (from 1540–1720 cm<sup>-1</sup>), and sebaceous regions of the fingermark were visualised using the integrated area under the band from 1713–1773 cm<sup>-1</sup>. Skin

**Table 3** Tentative assignment of FTIR bands observed in fingermarks<sup>5</sup>

Wavenumber (cm <sup>-1</sup> )	Band assignment	Putative chemical origin	Source
1375	CH <sub>3</sub> symmetric bend	Aliphatic carbon chains	Eccrine and sebaceous
1464	CH <sub>2</sub> symmetric bend	Aliphatic carbon chains	Sebaceous
1540–1700	O–H bend/N–H bend	Water, lactic acid or urea	Eccrine
1500–1700 (two peaks, 1650 and 1550)	Amide I & amide II	Protein	Skin debris
1712	C=O stretch in different environments	Saturated esters	Sebaceous
1745	C=O stretch	Saturated esters	Sebaceous
2854	CH <sub>2</sub> symmetric stretch	Long aliphatic carbon chains	Sebaceous
2927	CH <sub>3</sub> symmetric stretch	Long aliphatic carbon chains	Eccrine and sebaceous
2955	CH <sub>3</sub> asymmetric stretch (sh)	Fatty acids, glycerides and wax esters	Sebaceous
2980	CH <sub>3</sub> stretching	Aliphatic carbon chains	Eccrine
3009	Unsaturated =CH stretch	Squalene, unsaturated fatty acids, glycerides and wax esters	Sebaceous
~3400	O–H stretch	Water	Eccrine



Table 4 Tentative assignment of Raman bands observed in fingermarks<sup>36–46</sup>

Wavenumber (cm <sup>-1</sup> )	Band assignment	Putative chemical origin	Source
539	S–S stretching	Sulphur containing amino acids and proteins	Eccrine
773	Ring breathing	Phenylalanine	Eccrine
861	<i>para</i> -Substituted ring vibration	Tyrosine	Eccrine
929	C–C <sub>α</sub>	Protein backbone	Eccrine
1000	Ring breathing	Phenylalanine	Eccrine
1045	Ring deformation	Phenylalanine	Eccrine
1080	C–C stretching	Aliphatic carbon chains	Sebaceous
1091	O–P–O symmetric stretching	Nucleic acid backbone	Membrane lipids
1127	C–C stretching	Aliphatic carbon chains	Sebaceous
1173	C–C stretching	Aliphatic carbon chains	Sebaceous
1265	=CH deformation	Squalene, unsaturated fatty acids, glycerides and wax esters	Sebaceous
1300	CH <sub>2</sub> twisting	Aliphatic carbon chains	Sebaceous
1300	Amide III	Amino acids and proteins	Eccrine
1360	CH <sub>2</sub> deformation	Aliphatic carbon chains	Eccrine
1426	Ring stretching	Indole	Eccrine
1440	CH <sub>2</sub> and CH <sub>3</sub> deformation	Aliphatic carbon chains	Sebaceous
1457	CH <sub>2</sub> and CH <sub>3</sub> deformation	Aliphatic carbon chains	Sebaceous
1605	Ring C=C stretching	Histidine	Exogenous
1638	C=C symmetric stretching	Squalene, unsaturated fatty acids, glycerides and wax esters	Sebaceous
1652	Amide I	Amino acids and proteins	Eccrine
1660	C=C symmetric stretching	Squalene, unsaturated fatty acids, glycerides and wax esters	Sebaceous
1719	C=O stretching	Aldehydes	Sebaceous
1745	C=O stretching	Esters	Sebaceous
2725	Aliphatic CH stretching	Amino acids and proteins	Eccrine and sebaceous
2855	CH <sub>2</sub> symmetric stretching	Fatty acids and waxes	Sebaceous
2885	Fermi-resonance CH <sub>2</sub> stretching	Fatty acids and waxes	Sebaceous
2903	CH <sub>2</sub> asymmetric stretching	Fatty acids and waxes	Sebaceous
2930	Chain-end CH <sub>3</sub> symmetric stretching	Amino acids and proteins	Eccrine and sebaceous
2959	Chain-end CH <sub>3</sub> asymmetric stretching	Amino acids, proteins and aliphatic side-chains	Eccrine and sebaceous
3010	Unsaturated =CH stretching	Squalene, unsaturated fatty acids, glycerides and wax esters	Sebaceous
3330	O–H stretching	Water	Eccrine

debris was visualised using the integrated area under the band from 1507–1548 cm<sup>-1</sup> (amide II). Using these spectroscopic markers, the distribution of eccrine material, sebaceous material and skin debris across the fingermark ridges can be seen in Fig. 2. The images reveal a heterogeneous distribution of eccrine and sebaceous material across fingermark ridges, which appears to be segregated with little overlap between eccrine material (blue component, Fig. 2C) and sebaceous material (red component, Fig. 2C).

The results shown in Fig. 2 clearly demonstrate the heterogeneous distribution of eccrine components, which appear dispersed throughout the more abundant sebaceous material forming the ridges of the deposit. The variable distribution of eccrine and sebaceous components shown in Fig. 2 may help in accounting for some of the previous inconsistent findings in the literature. For example, Girod *et al.* reported identification of some IR bands due to eccrine secretions using  $\mu$ ATR-FTIR; however, those bands were not consistently observed in all fresh fingermarks.<sup>5</sup> Based on the heterogeneous and irregular distribution of eccrine components across the sebaceous fingermark ridges presented in Fig. 2, if large regions of a fingermark are not sampled, it would be possible to sample sebaceous ridges that contain minimal eccrine material. Although the results of FTIR spectroscopic

imaging at 20  $\mu$ m spatial resolution suggest segregation between eccrine and sebaceous chemical components, it does not conclusively preclude the possibility of mixing at a micron-scale (*i.e.* oil-in-water or water-in-oil type emulsions). Therefore, higher-spatial resolution imaging techniques, such as SR-ATR-FTIR and Raman microscopy, were used to investigate the homogeneity of sebaceous or eccrine-rich regions of the fingermark at the micron-scale.

#### Investigating the distribution of eccrine and sebaceous material in natural fingermarks at the micro-scale using SR-ATR-FTIR

The relatively long wavelengths of light across the mid-infrared range (2–20  $\mu$ m) have traditionally precluded the technique from biochemical studies at the micron- or sub-micron scale. Fortunately, advances in the application of ATR-FTIR spectroscopy, using high refractive index Ge ATR crystals, provide new opportunities.<sup>47</sup>

For point mapping FTIR measurements with a Ge ATR crystal, this has the effect of not only reducing the beam focus size by four times, but also reducing the mapping step size by four times relative to the physical step motion of the sample stage. It is therefore possible to achieve an ATR focus



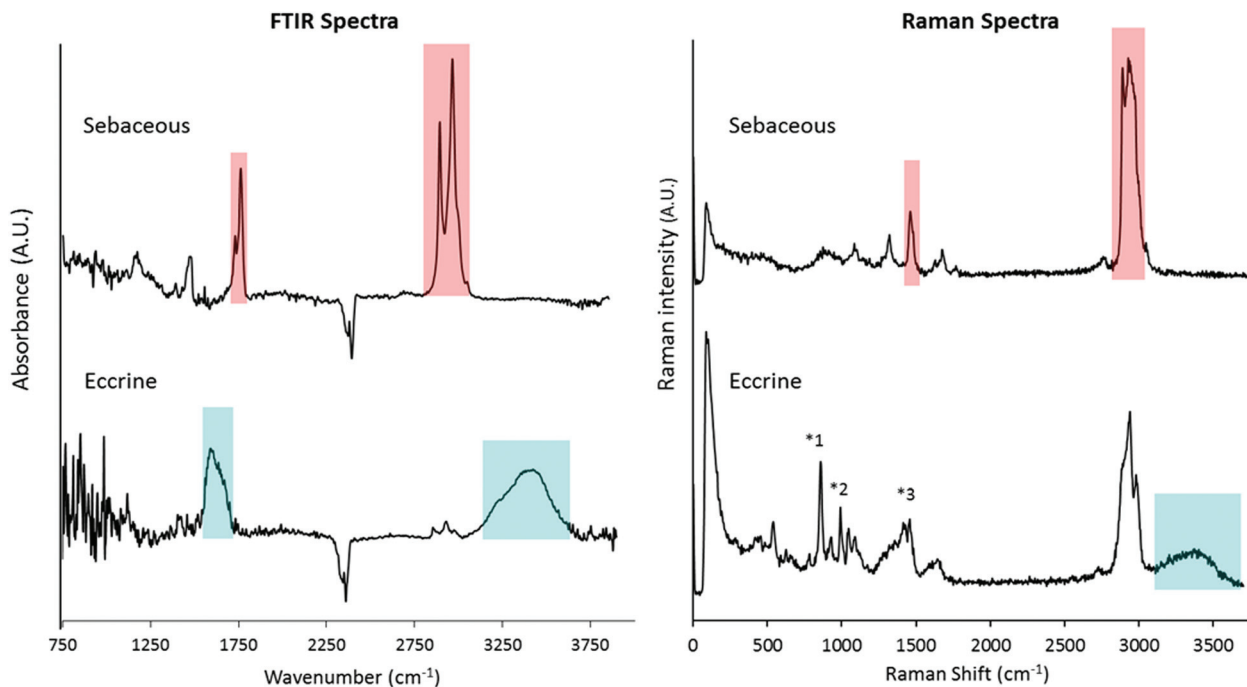


**Fig. 1** Comparison of transmission SR-FTIR and confocal Raman spectra of sebaceous and eccrine secretions. Red shaded regions represent bands characteristic of the sebaceous material and cyan shaded regions represent bands characteristic of the eccrine material. The marked Raman peaks, 1: 860  $\text{cm}^{-1}$ , 2: 1000  $\text{cm}^{-1}$  and 3: 1456  $\text{cm}^{-1}$ , were frequently encountered, which indicate a mixture of several amino acids/proteins present within an eccrine droplet.

spot size of around 2  $\mu\text{m}$  and a mapping step size of 0.25  $\mu\text{m}$ .<sup>47–49</sup>

In this study, ATR-FTIR spectroscopy was applied to image the distribution of eccrine and sebaceous material in individual droplets within fingerprint ridges. The minimum size of the infrared beam on the sample was 1.88  $\mu\text{m}$ , and the images were collected with a 0.25  $\mu\text{m}$  pixel size. A representative example of a ridge droplet imaged with ATR-FTIR and 0.25  $\mu\text{m}$  pixel size is shown in Fig. 3. Visual inspection of representative spectra (Fig. 3B) indicate that the droplet was composed primarily of sebaceous material (lipids), as confirmed by lipid distribution in the droplet (Fig. 3C). However, small regions ( $\sim 2\text{--}3$   $\mu\text{m}$  diameter) enriched with eccrine components and containing characteristic spectroscopic markers for water (Fig. 3B) were also observed (Fig. 3C). To a first approximation, the ATR-FTIR images of sebaceous and eccrine material reflect a water-in-oil emulsion. Therefore, although the majority of the droplet contained sebaceous material, in agreement with the segregation between eccrine and sebaceous material observed with FTIR imaging at the meso-scale, the higher spatial resolution of ATR-FTIR suggests that microscopic amounts of eccrine material can occur amongst sebaceous enriched regions.

A potential pitfall of ATR-FTIR is the requirement to bring the sample into physical contact with the ATR crystal, which may result in distortion of the shape of, or chemical distribution within, the droplet. However, in our studies, we found excellent agreement between the location and morphology of

fingerprint droplets in visible light images recorded before contact was made, and the infrared images after contact was made (ESI Fig. 1†). Furthermore, in a separate experiment, a natural fingerprint was deposited directly onto the tip of a Ge ATR crystal, which also revealed characteristic aqueous droplets adhered to the periphery of a larger sebaceous droplet (ESI Fig. 2†). While these results do not completely rule out the possibility of some distortion to droplet morphology or chemical distribution upon contact with the crystal, at the spatial resolution of the observations, the shape of the droplets and the relative distribution of fingerprint components within them appear to be unchanged.

#### Investigating the distribution of eccrine and sebaceous material in natural fingerprints at the micro-scale using confocal Raman microscopy

Although SR-ATR-FTIR enabled visualisation of eccrine and sebaceous components at the micron-scale, within individual droplets of natural fingerprints, the technique is limited by long collection times (several hours per image) and the requirement of a synchrotron light source. Thus, analysis of a larger data set was not possible. To further investigate the sub-micron distribution of sebaceous and eccrine material within individual droplets that compose fingerprint ridges, confocal Raman microscopy was used. Raman spectroscopy is complementary to FTIR in the detection of functional group vibrations. Due to the shorter wavelengths of light used in Raman spectroscopy, the technique provides improved spatial



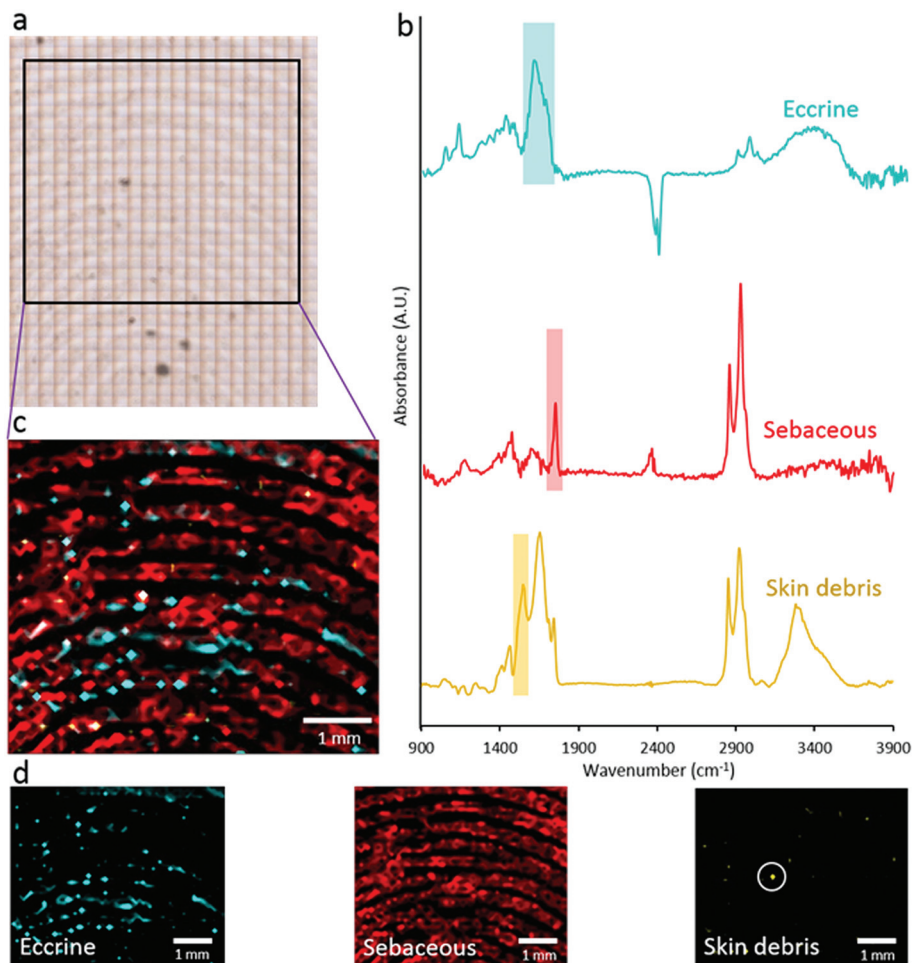


**Fig. 2** Bright field optical image of the area investigated with FTIR-FPA imaging (a) and FTIR spectra of eccrine (cyan), sebaceous (red) secretions and skin debris (yellow) obtained using the conventional FTIR spectroscopy (b). The composite distribution map (c) and individual false colour images were generated by integrating over the O–H bending band for the eccrine material (1520–1719 cm<sup>-1</sup>), the C=O band for the sebaceous material (1713–1773 cm<sup>-1</sup>) and the amide II band (1507–1548 cm<sup>-1</sup>) for skin debris (d). Spectral intensities are not scaled to the same y axis.

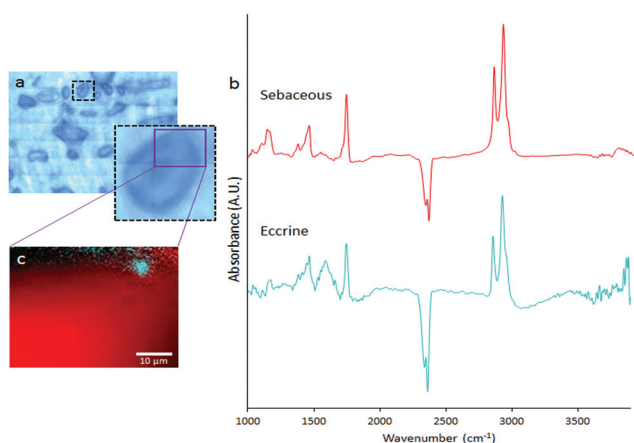


**Fig. 3** Bright field optical image of the area investigated with SR-ATR-FTIR (a) and FTIR spectra of eccrine (cyan) and sebaceous (red) secretions obtained using a synchrotron sourced IR microscope (b). The composite distribution map (c) was generated by integrating over the O–H bending band for eccrine (1500–1700 cm<sup>-1</sup>) and the C=O band for sebaceous (1713–1773 cm<sup>-1</sup>) secretions.

resolution (~250 nm) with 532 nm laser excitation and 100×, NA 0.9 objective, relative to FTIR.

**Natural fingermark deposits.** To further confirm the results observed with SR-ATR-FTIR, individual droplets along ridges of natural fingermarks were imaged with confocal Raman microscopy. A representative example from an 80 μm × 80 μm area of a natural fingermark deposit (from Donor 9) is shown in Fig. 4. The findings are in good agreement with those from SR-ATR-FTIR, and reveal fingermark droplets enriched in sebaceous material, containing localised regions enriched in eccrine material. In addition, due to the quick speed of data collection with Raman microscopy, larger regions of the fingermark were able to be imaged, which revealed the presence of eccrine enriched droplets containing small highly localised regions of sebaceous material. Taken together, the results from SR-ATR-FTIR and confocal Raman microscopy from this study support the distribution of eccrine and sebaceous material in fingermarks as water-in-oil or oil-in-water emulsions (investigated further in eccrine fingermarks, below).



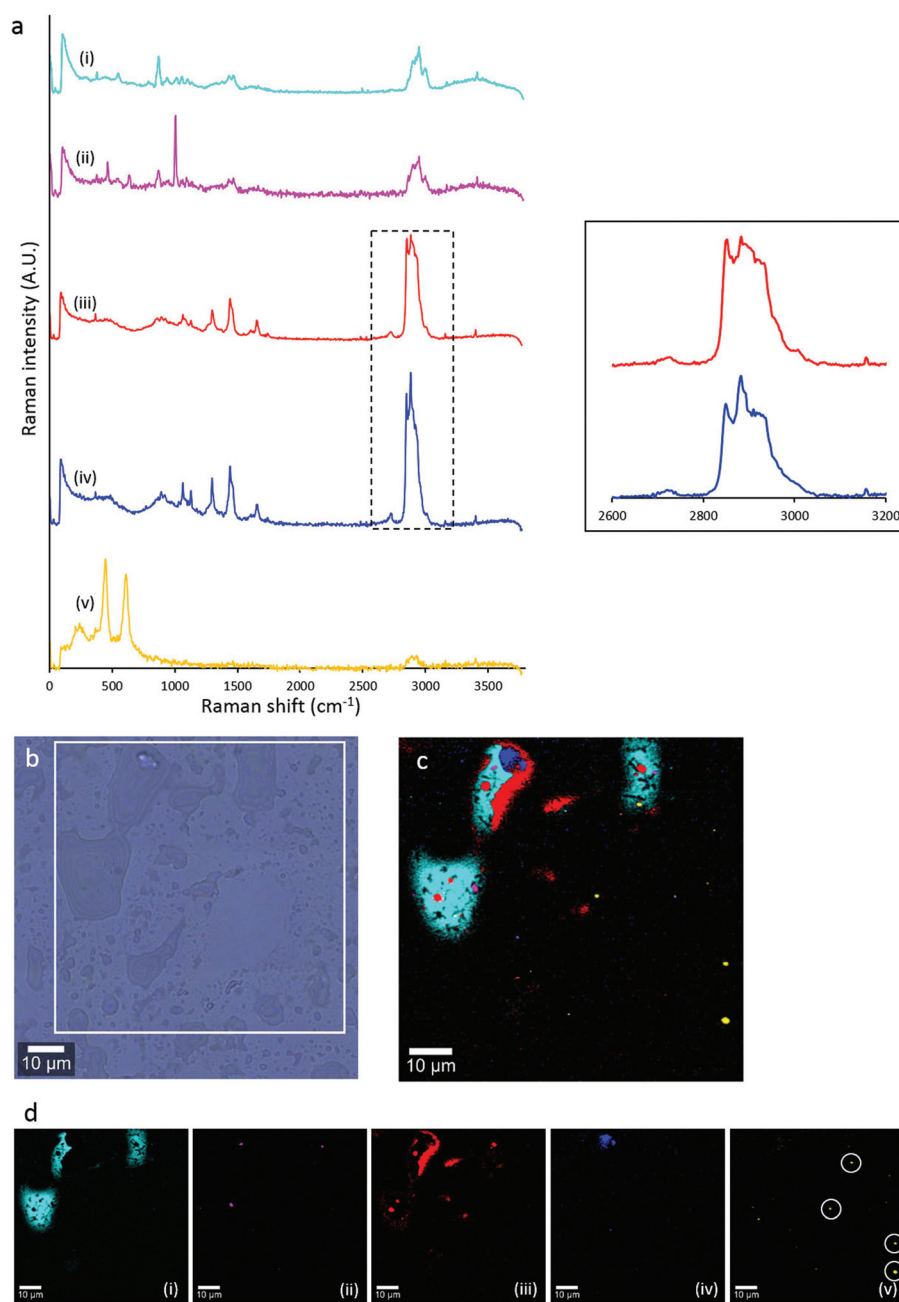


**Fig. 4** Averaged Raman spectra of the five components identified in a natural fingermark deposit from Donor 9 (a), bright field optical image of the area investigated (b), composite distribution map of the five components (c), and their distribution in false colours (d). The high wavenumber regions of the components (iii) and (iv) are expanded in a separate box to demonstrate the subtle differences in this region. The spatial distribution of component (v) is circled in (d) to aid the reader.

In addition to investigating the distribution of sebaceous and eccrine material within fingermark droplets, confocal Raman microscopy revealed five different chemical components within the droplets. Distinction between different lipid mixtures in the fingermark was achieved based on the spectral dissimilarities in the high wavenumber region ( $\sim 2850\text{--}3000\text{ cm}^{-1}$ , red shaded area in the Raman spectrum of sebaceous material, Fig. 1). The difference of intensity between both  $\text{CH}_2$  symmetric stretching ( $2855\text{ cm}^{-1}$ ) and the Fermi

resonance  $\text{CH}_2$  stretching ( $2886\text{ cm}^{-1}$ ) bands of component (iii) was not as large as in component (iv). The peak height ratio,  $I_{2886}/I_{2850}$ , is an indication of the intramolecular chain disorder and lateral packing between lipid acyl chains, with a lower band intensity ratio indicating a lower hydrocarbon chain order.<sup>38</sup> Future work will now investigate variation in lipid composition within sebaceous rich regions in natural fingermarks.

**Eccrine fingermark deposits.** As revealed in Fig. 4, within natural fingermark deposits, individual droplets enriched in



sebaceous components appear to contain microscopic amounts of eccrine material. Additionally, droplets enriched in eccrine material appear to contain microscopic amounts of sebaceous material (*i.e.* the droplets resemble a water-in-oil or oil-in-water emulsion, respectively). The occurrence of small lipid droplets within eccrine enriched regions of natural fingermarks raises the possibility that such observations could occur if small amounts of lipid exist in eccrine fingermarks. To investigate this in more detail, confocal Raman microscopy was used to investigate the distribution of eccrine and sebaceous material in “eccrine deposits” (*i.e.* deposits obtained after washing hands). As can be seen in Fig. 5, confocal Raman microscopy reveals multiple individual lipid droplets ( $\sim 0.2\text{--}0.5\ \mu\text{m}$  in diameter) that exist in a primarily eccrine matrix, within individual droplets of an “eccrine fingermark”.

### Significance and impact of the findings

The results of this study have revealed that while segregation between eccrine and sebaceous components is evident at the macroscopic level (*i.e.* meso-spatial resolution,  $\sim 20\ \mu\text{m}$ , as shown in Fig. 2), at the micron scale, sebaceous-rich fingermark regions frequently contain small amounts of eccrine material, and eccrine-rich fingermark regions contain small amounts of sebaceous material. Thus, at the microscopic scale, individual droplets that compose fingermark ridges reflect water-in-oil or oil-in-water emulsions. Considering that it is well established that fingermarks contain both eccrine and sebaceous material, this result may seem intuitive. However, to our knowledge, this is the first study to simultaneously detect and spatially localise both eccrine and sebaceous chemical components at micron resolution. Therefore,

this study provides the first strong, direct evidence supporting a long-held hypothesis in the field that the chemical composition and distribution of chemical components within fingermarks reflect water-in-oil and oil-in-water emulsions. As such, the results of this study have several important implications in the field of forensic science and fingermark detection.

Firstly, a recent detailed review of the occurrence and abundance of eccrine and sebaceous material in fingermarks highlighted the need for greater research into the distribution of these components in fingermarks.<sup>50</sup> It was previously thought that natural fingermarks were primarily comprised of eccrine material, with sebaceous components representing only a minor fraction.<sup>51</sup> Such a hypothesis largely arises from the fact that sebaceous glands are not present on the fingertips, and therefore, only minute quantities of sebaceous material are acquired from habitual touching of other body regions containing sebaceous glands (*i.e.* face, hair, or neck). However, as outlined by Kent,<sup>51</sup> much of the literature in the field does not support a primarily eccrine composition in natural fingermarks, with sebaceous components likely existing in much higher quantities than previously thought. The results of this study provide strong, direct evidence supporting the discussion by Kent, as we have directly demonstrated an abundance of sebaceous (lipid rich) material in natural fingermarks, and even in “eccrine fingermarks” collected after hand-washing. The source of the lipids in eccrine fingermarks remains to be confirmed; however, it is likely to be due to sebaceous material from other parts of the body that is not removed by hand-washing, with contributions from cellular-sourced lipids also possible. Ferguson *et al.* previously investigated peptides and proteins in fingermarks by MALDI-MSI, where the donors’ hands were cleaned with a 50% aqueous ethanol solution prior to deposition of eccrine-enriched fingermarks.<sup>13</sup> Yet, they putatively identified some anti-microbial peptides, which are found in sebaceous glands, suggesting that hand-washing does not completely remove all sebaceous material that has been transferred to the fingertips from other parts of the body.<sup>13</sup> Thus, our findings in combination with those of Ferguson *et al.* suggest that the complete removal of sebaceous material from fingers is difficult to achieve regardless of the use of soaps or solvents. This highlights a strong likelihood that lipids will be present at some level in all fingermarks in a forensic setting, and that developing and optimising fingermark detection methods targeted toward sebaceous components is a logical strategy.

The existence of a substantial amount of lipids in eccrine fingermarks also helps explain previously unexpected results in the field of fingermark detection.

For example, Wei *et al.* recently reported a latent fingermark development technique that makes use of the hydrophobic nature of the deposit to enhance the action of a hydrophilic dye that selectively binds to a bare cellulose membrane.<sup>52</sup> They reported that the technique offered satisfactory results even with eccrine fingermarks, which at the time were thought to be almost purely hydrophilic deposits. Our research demonstrates the presence of lipid droplets within eccrine deposits,

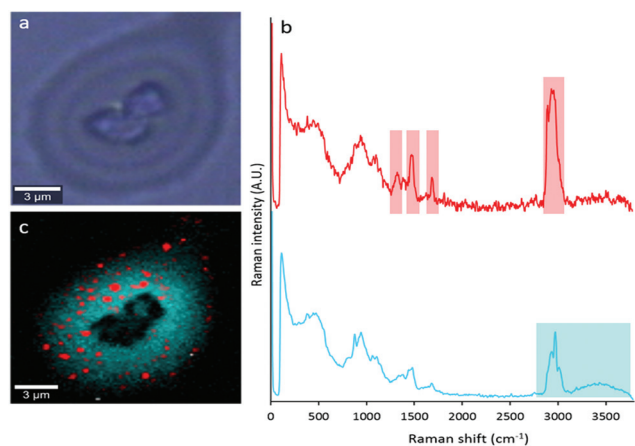


**Fig. 5** Bright field optical image of a droplet from an eccrine deposit imaged with confocal Raman microscopy (a), averaged Raman spectra of the two components identified in the droplet, blue shading highlights characteristic eccrine spectral features, and red shading highlights characteristic sebaceous spectral features (b) and its composite distribution map showing the distribution of the two components (c). The centre of the droplet in (a) is thought to be a small crystal of salt as no Raman bands were observed in that region other than very weak CH stretching bands. Spectra are scaled to the same y axis. Spectral differences are highlighted in shaded boxes.



which provides a mechanism accounting for the success of a hydrophobic-dependent detection technique when applied to primarily eccrine material. We demonstrate this effect further, and provide an example (Fig. 6), where successful visualisation of eccrine-enriched fingermarks is easily achieved using the lipophilic reagent Oil Red O.

The physical developer technique is the only technique that is currently used routinely in casework to develop fingermarks on wetted porous surfaces.<sup>43</sup> De la Hunty *et al.* suggested that PD may target a defined mixture of eccrine and lipid constituents, where both must be present in the deposit for silver deposition to occur.<sup>53,54</sup> They also emphasised the necessity to understand the state in which these targets are present, that is, as a mixture of various compounds or as an emulsion. Although our results are based on non-porous surfaces, they offer insights into this query as our study demonstrates evidence of fingermark droplets existing as an emulsion-like state, reflecting the amount of lipid and eccrine secretions in the droplet.

Our study also has implications for interpreting past studies investigating chemical alterations to fingermarks that occur with time following deposition, and for future experimental design of such studies. The heterogeneity observed at the micron scale in this study highlights that time-course studies, in which spatially resolved methods are developed, need to sample the identical/equivalent location of the fingermark across time. Failure to do so may result in observation of substantial variation across time-course measurements, the source of which may arise from spatial-derived-sample heterogeneity rather than time-course chemical alterations. For example, previous studies have combined FTIR spectroscopy

with chemometrics to infer donor traits and time since deposition by investigating the chemical changes of the fingermark deposit over time.<sup>5,14</sup> However, Fritz *et al.* failed to establish any trends over time with respect to donor traits and time since deposition, due to large uncertainties involved with the data. Our findings suggest that apart from the inter-donor variation, this large uncertainty may also be due to chemical heterogeneity across the deposit.

Lastly, our confirmation of the presence of lipids within eccrine droplets at the micron and sub-micron scale has validated the results of fingermark surface adhesion studies.<sup>21</sup> We previously investigated the surface adhesion of eccrine fingermark droplets using AFM with hydrophilic silicon cantilever tips and detected very low values (even negative values) for adhesion in some eccrine droplets.<sup>21</sup> Similarly, low values were observed on natural and sebaceous droplets which contained high amounts of lipids.<sup>21</sup> We were unable to explain this result at that time, but our current findings using *in situ* chemical analysis may now offer a possible explanation. Specifically, the findings of this current study suggest that previous AFM measurements were influenced by the presence of lipids, accounting for the similarity observed between results across natural and eccrine fingermarks.

## Conclusions

The results of this study advance our current understanding of the spatial distribution of sebaceous and eccrine chemical components within fingermarks. Specifically, the application of complementary sub-micron spatial resolution confocal Raman microscopy and sub-micron pixel resolution ATR-FTIR microscopy has provided definitive proof that fingermark droplets have a complex chemical composition of hydrophilic and hydrophobic components, and closely resemble an emulsion. A limitation of this study is the relatively small sample size analysed, which precludes conclusions to be drawn in a forensic context. Likewise, the fingermarks in this study were all analysed within 5 hours of deposition, which is too short a time frame for many forensic scenarios. Thus, the findings of this study should be viewed in the context of increasing the fundamental understanding of fingermark chemical composition, rather than in a forensic crime scene context. However, even with a small donor sample set, through extensive analysis of droplets, we demonstrate here for the first time that depending on the ratio of eccrine to sebaceous material in droplets, the droplets are likely to exist across a range including totally aqueous (eccrine), lipids in an aqueous matrix, aqueous droplets in a lipid matrix, or totally lipid droplets. Intriguingly, we observe a prominent presence of lipids across natural deposits, which were previously considered to contain a substantial amount of eccrine material. Recent discussions in the field have challenged the theory that natural deposits are primarily eccrine, and our results provide key direct evidence supporting these discussions. Our observation of the presence of lipids in microscopic amounts within eccrine enriched deposits pro-

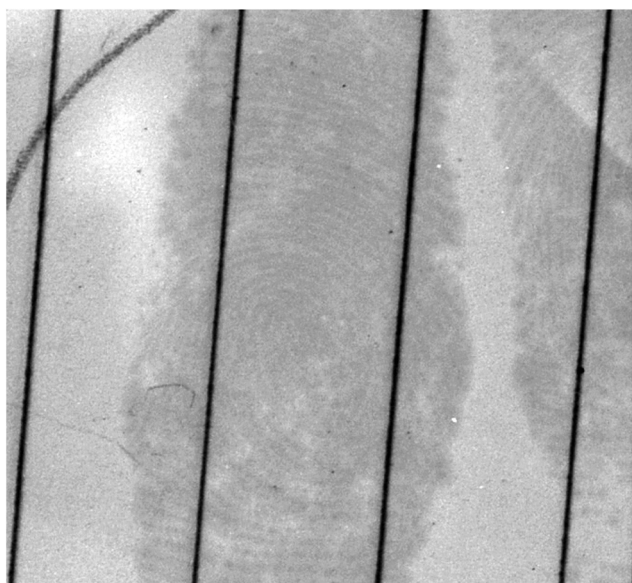


**Fig. 6** An eccrine fingermark on paper developed with Oil Red O. Development can be attributed to the occurrence of lipids in "eccrine deposits". (The colour and the contrast of the image were adjusted using Adobe Photoshop CC software to enhance the ridge details.)



vides a rationale for the success of lipophilic detection reagents when used on eccrine fingermarks. Lastly, this study provides the foundation for future studies to employ direct chemical imaging on a micron scale to study latent fingerprint chemical composition, which is critical to expand and develop current methodologies for fingerprint detection.

This study has been approved by the Curtin University Human Research Ethics Committee (Approval Number RDSE-02-15). Informed consent was obtained from all human subjects.

## Conflicts of interest

The authors declare no competing financial interest.

## Acknowledgements

Part of this research was undertaken on the Infrared Microspectroscopy Beamline at the Australian Synchrotron, part of ANSTO, and WITec GmbH, Ulm, Germany. We acknowledge travel funding provided by the Synchrotron Access Program, managed by the Australian Synchrotron, part of ANSTO, and funded by the Australian Government. Thanks go to the Australian Synchrotron and WITec GmbH staff for their expert opinions and support. The authors acknowledge Dr Stefan Gomes da Costa, Dr Thomas Dieing, Dr Henning Dampel and Matthias Kress from WITec GmbH for their useful discussions on the manuscript. The authors would like to acknowledge the contribution of an Australian Government Research Training Program Scholarship in supporting this research. The authors would like to thank all the fingerprint donors for their cooperation.

## References

- 1 S. Moret, X. Spindler, C. Lennard and C. Roux, Microscopic examination of fingerprint residues: Opportunities for fundamental studies, *Forensic Sci. Int.*, 2015, **255**, 28–37.
- 2 G. M. Mong, C. Petersen and T. Clauss, *Advanced fingerprint analysis project fingerprint constituents*, Pacific Northwest National Lab., Richland, WA, US, 1999.
- 3 N. E. Archer, Y. Charles, J. A. Elliott and S. Jickells, Changes in the lipid composition of latent fingerprint residue with time after deposition on a surface, *Forensic Sci. Int.*, 2005, **154**(2), 224–239.
- 4 K. A. Mountfort, H. Bronstein, N. Archer and S. M. Jickells, Identification of Oxidation Products of Squalene in Solution and in Latent Fingerprints by ESI-MS and LC/APCI-MS, *Anal. Chem.*, 2007, **79**(7), 2650–2657.
- 5 A. Girod, L. Xiao, B. Reedy, C. Roux and C. Weyermann, Fingerprint initial composition and aging using Fourier transform infrared microscopy ( $\mu$ -FTIR), *Forensic Sci. Int.*, 2015, **254**, 185–196.
- 6 A. A. Frick, *Chemical investigations into the lipid fraction of latent fingerprint residue*, PhD Thesis, Curtin University, 2015.
- 7 P. Fritz, *Chemical studies into the amino acids present in latent fingerprints*, PhD Thesis, Curtin University, Perth, 2015.
- 8 A. Girod and C. Weyermann, Lipid composition of fingerprint residue and donor classification using GC/MS, *Forensic Sci. Int.*, 2014, **238**, 68–82.
- 9 G. Thomas, The physics of fingerprints and their detection, *J. Phys. E: Sci. Instrum.*, 1978, **11**(8), 722–731.
- 10 M. Tahtouh, J. R. Kalman, C. Roux, C. Lennard and B. J. Reedy, The detection and enhancement of latent fingerprints using infrared chemical imaging, *J. Forensic Sci.*, 2005, **50**(1), JFS2004213–9.
- 11 S. G. Kazarian and K. A. Chan, ATR-FTIR spectroscopic imaging: recent advances and applications to biological systems, *Analyst*, 2013, **138**(7), 1940–1951.
- 12 R. Wolstenholme, R. Bradshaw, M. Clench and S. Francese, Study of latent fingerprints by matrix-assisted laser desorption/ionisation mass spectrometry imaging of endogenous lipids, *Rapid Commun. Mass Spectrom.*, 2009, **23**(19), 3031–3039.
- 13 L. S. Ferguson, F. Wulfert, R. Wolstenholme, J. M. Fonville, M. R. Clench, V. A. Carolan and S. Francese, Direct detection of peptides and small proteins in fingerprints and determination of sex by MALDI mass spectrometry profiling, *Analyst*, 2012, **137**(20), 4686–4692.
- 14 P. Fritz, W. Bronswijk, K. Lepkova, S. Lewis, D. Martin and L. Puskar, Infrared microscopy studies of the chemical composition of latent fingerprint residues, *Microchem. J.*, 2013, **111**, 40–46.
- 15 C. Ricci, P. Phiriyavityopas, N. Curum, K. A. Chan, S. Jickells and S. G. Kazarian, Chemical imaging of latent fingerprint residues, *Appl. Spectrosc.*, 2007, **61**(5), 514–522.
- 16 E. Bartick, R. Schwartz, R. Bhargava, M. Schaeberle, D. Fernandez and I. Levin, Spectrochemical analysis and hyperspectral imaging of latent fingerprints, in *16th Meeting of the International Association of Forensic Sciences*, 2002, pp. 61–64.
- 17 D. K. Williams, R. L. Schwartz and E. G. Bartick, Analysis of latent fingerprint deposits by infrared microspectroscopy, *Appl. Spectrosc.*, 2004, **58**(3), 313–316.
- 18 N. J. Crane, E. G. Bartick, R. S. Perlman and S. Huffman, Infrared spectroscopic imaging for noninvasive detection of latent fingerprints, *J. Forensic Sci.*, 2007, **52**(1), 48–53.
- 19 K. M. Antoine, S. Mortazavi, A. D. Miller and L. M. Miller, Chemical differences are observed in children's versus adults' latent fingerprints as a function of time, *J. Forensic Sci.*, 2010, **55**(2), 513–518.
- 20 D. K. Williams, C. J. Brown and J. Bruker, Characterization of children's latent fingerprint residues by infrared microspectroscopy: Forensic implications, *Forensic Sci. Int.*, 2011, **206**(1), 161–165.
- 21 B. N. Dorakumbura, T. Becker and S. W. Lewis, Nanomechanical mapping of latent fingerprints: A preliminary



- nary investigation into the changes in surface interactions and topography over time, *Forensic Sci. Int.*, 2016, **267**, 16–24.
- 22 R. M. Connatser, S. M. Prokes, O. J. Glembocki, R. L. Schuler, C. W. Gardner, S. A. Lewis and L. A. Lewis, Toward Surface-Enhanced Raman Imaging of Latent Fingerprints, *J. Forensic Sci.*, 2010, **55**(6), 1462–1470.
- 23 W. Song, Z. Mao, X. Liu, Y. Lu, Z. Li, B. Zhao and L. Lu, Detection of protein deposition within latent fingerprints by surface-enhanced Raman spectroscopy imaging, *Nanoscale*, 2012, **4**(7), 2333–2338.
- 24 J. S. Day, H. G. Edwards, S. A. Dobrowski and A. M. Voice, The detection of drugs of abuse in fingerprints using Raman spectroscopy I: latent fingerprints, *Spectrochim. Acta, Part A*, 2004, **60**(3), 563–568.
- 25 J. S. Day, H. G. Edwards, S. A. Dobrowski and A. M. Voice, The detection of drugs of abuse in fingerprints using Raman spectroscopy II: cyanoacrylate-fumed fingerprints, *Spectrochim. Acta, Part A*, 2004, **60**(8), 1725–1730.
- 26 H. J. Byrne, G. D. Sockalingum and N. Stone, Raman Microscopy: Complement or Competitor?, in *Biomedical Applications of Synchrotron Infrared Microspectroscopy*, 2010, vol. 11, pp. 105–142.
- 27 G. Socrates, *Infrared and Raman characteristic group frequencies: tables and charts*, John Wiley & Sons, 2004.
- 28 M. Puit, M. Ismail and X. Xu, LCMS Analysis of Fingerprints, the Amino Acid Profile of 20 Donors, *J. Forensic Sci.*, 2014, **59**(2), 364–370.
- 29 A. Frick, G. Chidlow, S. Lewis and W. Van Bronswijk, Investigations into the initial composition of latent fingerprint lipids by gas chromatography–mass spectrometry, *Forensic Sci. Int.*, 2015, **254**, 133–147.
- 30 M. V. Buchanan, K. Asano and A. Bohanon, *Chemical characterization of fingerprints from adults and children*, Oak Ridge National Lab., TN, United States, 1996.
- 31 C. Weyermann, C. Roux and C. Champod, Initial results on the composition of fingerprints and its evolution as a function of time by GC/MS analysis, *J. Forensic Sci.*, 2011, **56**(1), 102–108.
- 32 A. Frick, G. Chidlow, J. Goodpaster, S. Lewis and W. van Bronswijk, Monitoring compositional changes of the lipid fraction of fingerprint residues deposited on paper during storage, *Forensic Chem.*, 2016, **2**, 29–36.
- 33 R. K. Freinkel and D. T. Woodley, *The biology of the skin*, CRC Press, 2001.
- 34 R. S. Croxton, M. G. Baron, D. Butler, T. Kent and V. G. Sears, Variation in amino acid and lipid composition of latent fingerprints, *Forensic Sci. Int.*, 2010, **199**(1), 93–102.
- 35 A. Girod, R. Ramotowski and C. Weyermann, Composition of fingerprint residue: A qualitative and quantitative review, *Forensic Sci. Int.*, 2012, **223**(1), 10–24.
- 36 J. De Gelder, K. De Gussem, P. Vandenabeele and L. Moens, Reference database of Raman spectra of biological molecules, *J. Raman Spectrosc.*, 2007, **38**(9), 1133–1147.
- 37 C. Krafft, T. Knetschke, R. H. Funk and R. Salzer, Identification of organelles and vesicles in single cells by Raman microspectroscopic mapping, *Vib. Spectrosc.*, 2005, **38**(1), 85–93.
- 38 D. Borchman, D. Tang and M. C. Yappert, Lipid composition, membrane structure relationships in lens and muscle sarcoplasmic reticulum membranes, *Biospectroscopy*, 1999, **5**(3), 151–167.
- 39 A. L. Jenkins, R. A. Larsen and T. B. Williams, Characterization of amino acids using Raman spectroscopy, *Spectrochim. Acta, Part A*, 2005, **61**(7), 1585–1594.
- 40 C. Krafft, T. Knetschke, A. Siegner, R. H. Funk and R. Salzer, Mapping of single cells by near infrared Raman microspectroscopy, *Vib. Spectrosc.*, 2003, **32**(1), 75–83.
- 41 C. Matthäus, T. Chernenko, J. A. Newmark, C. M. Warner and M. Diem, Label-free detection of mitochondrial distribution in cells by nonresonant Raman microspectroscopy, *Biophys. J.*, 2007, **93**(2), 668–673.
- 42 B. Barry, H. Edwards and A. Williams, Fourier transform Raman and infrared vibrational study of human skin: assignment of spectral bands, *J. Raman Spectrosc.*, 1992, **23**(11), 641–645.
- 43 M. Langlais, H. A. Tajmir-Riahi and R. Savoie, Raman spectroscopic study of the effects of Ca<sup>2+</sup>, Mg<sup>2+</sup>, Zn<sup>2+</sup>, and Cd<sup>2+</sup> ions on calf thymus DNA: binding sites and conformational changes, *Biopolymers*, 1990, **30**(7–8), 743–752.
- 44 J. Neault, M. Naoui, M. Manfait and H. Tajmir-Riahi, Aspirin-DNA interaction studied by FTIR and laser Raman difference spectroscopy, *FEBS Lett.*, 1996, **382**(1–2), 26–30.
- 45 R. S. Das and Y. Agrawal, Raman spectroscopy: recent advancements, techniques and applications, *Vib. Spectrosc.*, 2011, **57**(2), 163–176.
- 46 G. Zhu, X. Zhu, Q. Fan and X. Wan, Raman spectra of amino acids and their aqueous solutions, *Spectrochim. Acta, Part A*, 2011, **78**(3), 1187–1195.
- 47 M. Tobin, K. R. Bamberg, D. E. Martin, L. Puskar, D. A. Beattie, E. P. Ivanova, S.-H. Nguyen, H. K. Webb and J. Vongsvivut, Attenuated Total Reflection FTIR Microspectroscopy at the Australian Synchrotron, in *Light, Energy and the Environment*, Leipzig, 2016/11/14, Optical Society of America, Leipzig, 2016, p. FTu2E.5.
- 48 M. Ryu, A. Balčytis, X. Wang, J. Vongsvivut, Y. Hikima, J. Li, M. J. Tobin, S. Juodkakis and J. Morikawa, Orientational mapping augmented sub-wavelength hyper-spectral imaging of silk, *Sci. Rep.*, 2017, **7**(1), 7419.
- 49 J. Vongsvivut, V. K. Truong, M. Al Kobaisi, S. Maclaughlin, M. J. Tobin, R. J. Crawford and E. P. Ivanova, Synchrotron macro ATR-FTIR microspectroscopic analysis of silica nanoparticle-embedded polyester coated steel surfaces subjected to prolonged UV and humidity exposure, *PLoS One*, 2017, **12**(12), e0188345.
- 50 S. Cadd, M. Islam, P. Manson and S. Bleay, Fingerprint composition and aging: A literature review, *Sci. Justice*, 2015, **55**(4), 219–238.
- 51 T. Kent, Water content of latent fingerprints—Dispelling the myth, *Forensic Sci. Int.*, 2016, **266**, 134–138.



- 52 Q. Wei, X. Li, X. Du, X. Zhang and M. Zhang, Universal and one-step visualization of latent fingermarks on various surfaces using hydrophilic cellulose membrane and dye aqueous solution, *Sci. China: Chem.*, 2017, 1–8.
- 53 M. de la Hunty, S. Moret, S. Chadwick, C. Lennard, X. Spindler and C. Roux, Understanding Physical Developer (PD): Part II—Is PD targeting eccrine constituents?, *Forensic Sci. Int.*, 2015, 257, 488–495.
- 54 M. de la Hunty, S. Moret, S. Chadwick, C. Lennard, X. Spindler and C. Roux, Understanding physical developer (PD): Part I—Is PD targeting lipids?, *Forensic Sci. Int.*, 2015, 257, 481–487.

